MPPT of Photovoltaic Systems using Extremum—Seeking Control

R. LEYVA
Universitat Rovira i Virgili
Spain

C. ALONSO

I. QUEINNEC

A. CID-PASTOR

D. LAGRANGE
LAAS-CNRS
France

L. MARTÍNEZ-SALAMERO
Universitat Rovira i Virgili
Spain

A stability analysis for a maximum power point tracking (MPPT) scheme based on extremum-seeking control is developed for a photovoltaic (PV) array supplying a dc-to-dc switching converter. The global stability of the extremum-seeking algorithm is demonstrated by means of Lyapunov's approach. Subsequently, the algorithm is applied to an MPPT system based on the "perturb and observe" method. The steady-state behavior of the PV system with MPPT control is characterized by a stable oscillation around the maximum power point. The tracking algorithm leads the array coordinates to the maximum power point by increasing or decreasing linearly with time the array voltage. Off-line measurements are not required by the control law, which is implemented by means of an analog multiplier, standard operational amplifiers, a flip-flop circuit and a pulsewidth modulator. The effectiveness of the proposed MPPT scheme is demonstrated experimentally under different operating conditions.

Manuscript received September 7, 2004; revised March 4, 2005; released for publication May 31, 2005.

IEEE Log No. T-AES/42/1/862549.

Refereeing of this contribution was handled by W. M. Polivka.

Authors' addresses: R. Leyva, and L. Martínez-Salamero, Dept. Eng. Electrònica, Elèctrica i Automàtica, Universitat Rovira i Virgili, Av. Països Catalans 26, 43007 Tarragona, Spain, E-mail: (rleyva@etse.urv.es); C. Alonso, I. Queinnec, A. Cid-Pastor, D. Lagrange, Laboratoire d'Analyse et d'Architecture des Systèmes, LAAS-CNRS, 7, Avenue du Colonel Roche, 31077 Toulouse, France.

I. INTRODUCTION

The conversion of solar energy into electric energy is performed by means of photovoltaic (PV) generators which supply electric current in the first quadrant of the current-voltage plane, particularly, in the voltage region located within the $[0, v_{OC}]$ interval, where v_{OC} is the open-circuit voltage. Parameter v_{OC} depends on the number of solar cells connected in series within the solar array, on the fabrication technology of the cell, and the temperature, while the supplied current depends on the solar insolation level. Figs. 1(a) and 1(b) depict the *i-v* (current-voltage) and *p-v* (power-voltage) characteristics of a solar array for different temperatures. Therefore, the power supplied by the PV array depends to a great extent on the atmospheric conditions.

The maximization of the power extracted from the PV array is usually carried out by means of mechanical and/or electronic systems. In the first case, sun tracking systems optimize the solar incidence angle while in the electronic approach a maximum power transfer at the PV array terminals is pursued by means of maximum power point tracking (MPPT) methods. Mechanical and electronic systems for power maximization are compatible and complementary requiring a measurement of the array operating conditions and a posterior adjustment if the external conditions change.

The reported solutions for MPPT in PV systems are based on different criteria. Some of them estimate the power-voltage or power-current characteristics minimizing the cost of the estimation. In a report representative of this technique due to Enslin, et al. [1], the v_{OC} parameter of the array is measured every 30 operation intervals. Then, assuming that the power peak is located at 76% of v_{OC}, the controller adapts the energy conversion. An efficiency analysis of each element of the PV generation system is also included, this eventually allowing to measure the global efficiency of the integrated solution developed by the authors. However, such approximation is not optimal since during 1 out of 30 intervals the panel does not generate energy. Moreover, the assumption of $0.76v_{OC}$ for the voltage coordinate of the maximum power point is only true for certain parameters of the curve. Also, the converter output has to cope with a big stress every 30 intervals during the system start-up. In a similar approach by Noguchi [2], the optimal output current of the array is adaptively estimated by taking into account the presence of disturbances such as partial shades in the panels. This technique requires the measurement of the short-circuit current, this also implying a big excursion through the *p-v* characteristics to estimate the maximum power value. Another approach is based on impedance matching, the works of Wyatt and Chua [3] being the most representative. In such

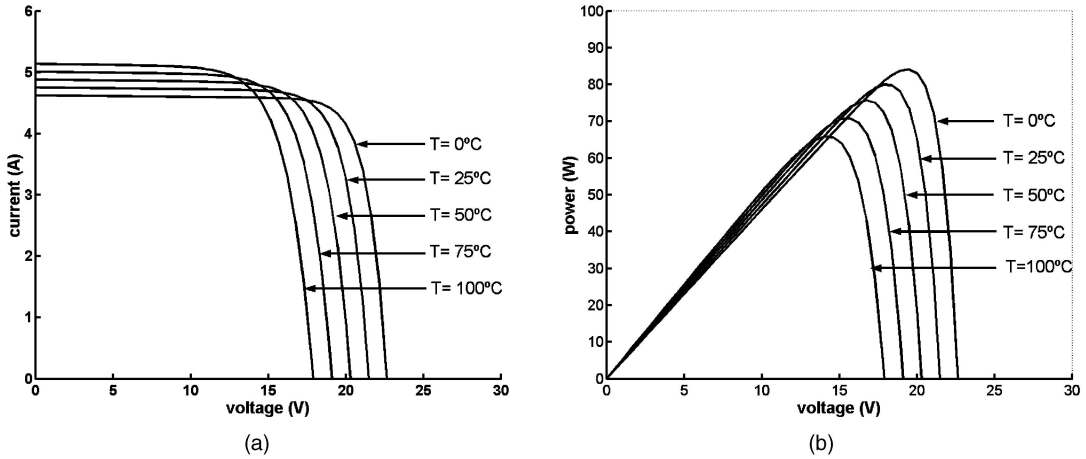

(a) (b)

Fig. 1. (a) Current-versus-voltage characteristics of PV array. (b) Power versus voltage.

case, the expression of the maximum power point is obtained by means of impedance matching and using the mathematical model of the solar cell. The main drawbacks of this technique are due to the absence of parametric uncertainty in the model and to the difficulty of adaptation to variable temperatures due to the big number of mathematical operations involved. The work of Appelbaum [4] on the comparison of two PV configurations for water pumping is also based on this technique.

A mixed technique of the previous methods is reported in [5] where the array parameters are extracted and subsequently used in a circuit model in which the maximum power point is eventually found.

Another strategy for searching the maximum power point is based on the extremum-seeking control theory which tries to establish a feedback system which produces an oscillatory behavior around the equilibrium point. This procedure does not require the estimated position of the maximum power point. The results reported in [6–9] belong to this category of MPPT systems. Other algorithms of extremum-seeking control insert a small sinusoidal perturbation and establish the control action as a function of the output system response [10]. This technique is called "perturb and observe" algorithm and it has been also employed in [11] in combination with impedance matching concepts. However, these algorithms intending the extremum-seeking control require a stability guarantee for the feedback system which in most of the cases has been experimentally verified but not analytically proved.

In this paper, an MPPT algorithm providing an efficient extraction of the PV array energy and ensuring the stability of the adjusting process for sudden or fast variations of the external conditions is presented. The paper is organized as follows. In Section II, the stability of an extremum-seeking generic problem is analyzed using Lyapunov's approach. Based on the results of Section II, a feedback scheme for maximum power extraction in a PV array is described in Section III. Experimental results for different operating conditions are shown in Section IV. Finally, conclusions are contained in Section V.

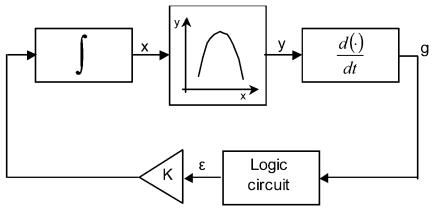

Fig. 2. Block diagram of extremum-seeking control system.

II. EXTREMUM SEEKING CONTROL

The foundations of extremum-seeking control can be found in the early 1920s in the work of Leblanc on the search of the resonance peak of an electromechanical system [10]. In the 1960s, there were also important contributions, among which the works of Korovin and Morosanov constitute the most significant advances [10]. The nonlinear and adaptive nature of such control is clearly shown in [14]. Although there are different extremum-seeking algorithms an important analytic effort should be made in order to establish the stability regions of a great number of reported applications [11].

The block diagram of an extremum-seeking problem is depicted in Fig. 2. The equations describing the system behavior are governed by an integrator,

$$\frac{dx}{dt} = K\varepsilon \qquad \text{where} \quad \varepsilon = \pm 1 \text{ and } K \text{ is a constant} \tag{1}$$

a differentiator

$$g = \frac{dy}{dt} \tag{2}$$

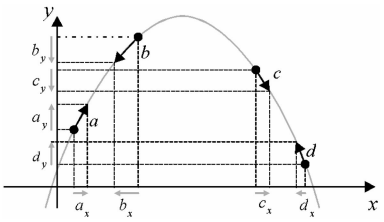

Fig. 3. Illustrative cases of extremum-seeking mechanism.

and a logic circuitry subsystem which implements the following function

$$\begin{array}{ll} \text{change the sign of } \varepsilon & \text{if} \quad g < 0 \\ \text{keep the sign of } \varepsilon & \text{if} \quad g > 0 \end{array}. \tag{3}$$

Fig. 3 summarizes the behavior of the extremum-seeking algorithm. Four cases can be distinguished.

Case 1 Vector a describes a movement where both horizontal and vertical components are increasing, i.e., $(dx/dt)|_{t^-} > 0$, $(dy/dt)|_{t^-} > 0$, which results in a trajectory directed towards the optimal point from its left side. Therefore, the controller must keep the sign of the horizontal variation, i.e., $(dx/dt)|_{t^+} = K$.

Case 2 Vector b describes a movement where both horizontal and vertical components are decreasing, i.e., $(dx/dt)|_{t^-} < 0$, $(dy/dt)|_{t^-} < 0$, which corresponds to a trajectory moving away from the optimal point towards the left. Hence, the logic circuitry must change the sign of the horizontal variation, i.e., $(dx/dt)|_{t^+} = K$.

Case 3 Vector c illustrates a movement where the horizontal component is increasing while the vertical component is decreasing, i.e., $(dx/dt)|_{t^-} > 0$, $(dy/dt)|_{t^-} < 0$, which represents a movement going away from the maximum point towards the right. The control action will change in this case the sign of the horizontal variation. Therefore, $(dx/dt)|_{t^+} = -K$.

Case 4 Vector d corresponds to a movement whose horizontal component is decreasing whereas its vertical component is increasing, i.e., $(dx/dt)|_{t^-} < 0$, $(dy/dt)|_{t^-} > 0$; this illustrates a trajectory directed to the optimal point from its right side. Therefore, the controller must keep the sign of the horizontal variation, i.e., $(dx/dt)|_{t^+} = -K$.

Since $dy/dx = (dy/dt)/(dx/dt)$, cases 1–4 can be expressed in compact form as follows

$$\left.\frac{dx}{dt}\right|_{t^+} = K \qquad \text{if} \quad \left.\frac{dy}{dx}\right|_{t^-} > 0 \tag{4}$$

$$\left.\frac{dx}{dt}\right|_{t^+} = -K \qquad \text{if} \quad \left.\frac{dy}{dx}\right|_{t^-} < 0. \tag{5}$$

Equations (4) and (5) can also be reduced to only one expression

$$\frac{dx}{dt} = K\,\text{sign}\left(\frac{dy}{dx}\right). \tag{6}$$

Note that the algorithm measures the sign of dy/dt, whereas the resulting dynamics are governed by dy/dx. Also, it can be observed in (6) that the equilibrium point $dx/dt = 0$ will correspond to an extremum of the x-y curve in Fig. 2, where $dy/dx = 0$. Note also in (6) that the system dynamics change with constant slope, which can be either positive or negative, this depending on the sign of the slope of the x-y curve.

In order to demonstrate that the equilibrium point is stable, a positive definite function $V(t)$ is defined in a concave domain of $y(x)$

$$V(t) = \frac{1}{2}\left(\frac{dy}{dx}\right)^2. \tag{7}$$

Hence

$$\dot{V}(t) = \frac{dy}{dx}\frac{d^2y}{dx^2}\frac{dx}{dt} = \frac{dy}{dx}\frac{d^2y}{dx^2}\left(K\,\text{sign}\left(\frac{dy}{dx}\right)\right). \tag{8}$$

The concavity of $y(x)$ implies

$$\frac{d^2y}{dx^2} < 0. \tag{9}$$

On the other hand,

$$\frac{dy}{dx}\text{sign}\left(\frac{dy}{dx}\right) > 0. \tag{10}$$

Therefore, choosing a positive value for K will imply $\dot{V}(t) < 0$, i.e., a negative definite function, which demonstrates the global stability of the system given by (6).

Since the v-p characteristics of a solar array is a concave function, the previous analysis can be applied to solve the problem of MPPT.

III. MPPT BASED ON EXTREMUM-SEEKING CONTROL

In the case of a solar array, the extremum-seeking algorithm will force the PV system to approach to the maximum power point by increasing or decreasing the voltage at the array terminals with a constant value of the time-derivative. To adapt the array voltage a dc-to-dc switching converter is inserted between the solar panel and a load (Fig. 4). In this case the converter load is a battery and the converter input signals are panel voltage v_{SA} and panel current i_{SA}. The variables x and y of the MPPT function depicted in Fig. 2 correspond in Fig. 4 to the panel voltage v_{SA} and the panel power p_{SA}, respectively (where $p_{\text{SA}} = i_{\text{SA}} \cdot v_{\text{SA}}$). The variation of v_{SA} with constant time-derivative is achieved by imposing such behavior to the converter duty cycle D.

A. Array Voltage Variation

The variation of the duty cycle changes input voltage V_{IN} of the converter and therefore the PV

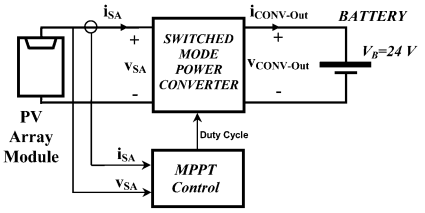

Fig. 4. MPPT scheme of PV system.

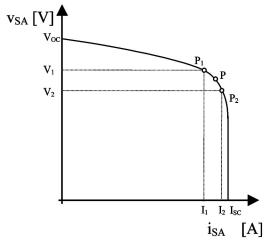

Fig. 5. PV panel operating points for different values of converter dc input voltage.

panel operating point as depicted in Fig. 5. In such figure the operating points P_1 and P_2 correspond, respectively, to input voltages V_{IN1} and V_{IN2} or equivalently to duty cycles D_1 and D_2. Without loss of generality, assume a boost structure as the power converter in Fig. 4. In that case, the expression of V_{IN} is given by

$$V_{IN} = V_B(1 - D) \tag{11}$$

where V_B is the battery voltage which is modeled as a constant value due to its slow charge dynamics.

Assume that the transition from P_1 to a generic point P is carried out by increasing the duty cycle as follows

$$D_P(t) = D_1 + \alpha t \qquad \text{where} \quad \alpha \text{ is a positive constant.} \tag{12}$$

Therefore, the expression of $V_P(t)$ is given by

$$V_P = V_B(1 - D_P) = V_B(1 - D_1 - \alpha). \tag{13}$$

On the other hand, $1 - D_P$ can be related to the coordinates of P_1

$$V_1 = V_B(1 - D_1). \tag{14}$$

Taking into account (14), (13) becomes

$$V_P(t) = V_B(1 - D_1 - \alpha t) = V_1 - V_B\alpha t. \tag{15}$$

Note that a transition involving a decrease of the duty cycle, i.e., a negative slope in (12) would imply a change of the sign of α in (15). Hence, (15) describes the linear decreasing with time of the voltage at the solar array terminals.

Similarly, a decrease in the duty cycle would result in an increase of $v_P(t)$ given by

$$V_P = V_1 + V_B\alpha t. \tag{16}$$

On the other hand, the derivative of the power P delivered by the solar array versus the duty cycle is given by

$$\frac{dP}{dD} = \frac{dP}{dV_{IN}}\frac{dV_{IN}}{dD}. \tag{17}$$

Taking into account (11), (17) becomes

$$\frac{dP}{dD} = -V_B\frac{dP}{V_{IN}}. \tag{18}$$

Hence,

$$\frac{d^2P}{dD^2} = -V_B\frac{d^2P}{dV_{IN}^2}\frac{dV_{IN}}{dD} = V_B^2\frac{d^2P}{dV_{IN}^2}. \tag{19}$$

At the maximum power point $dP/dV_{IN} = 0$, which implies

$$\frac{dP}{dD} = 0. \tag{20}$$

Also at maximum power point $d^2P/dV_{IN}^2 < 0$, which results in

$$\frac{d^2P}{dD^2} < 0. \tag{21}$$

From (20) and (21), we conclude that the solar array power is a concave function of the duty cycle. Therefore, the extremum-seeking algorithm can be applied directly on the converter duty cycle which controls the power panel. The search of the maximum power point would result in a trajectory through the *v-i* characteristics of the PV array characterized by a voltage triangular waveform in the time-domain with slopes $-V_B\alpha$ and $+V_B\alpha$ for the left to right and for the left to right movement, respectively.

B. MPPT Description

Fig. 6 shows the block diagram corresponding to the MPPT subsystem. The power supplied by the panel is calculated by means of an analog multiplier. This signal is processed by a linear circuit whose transfer function is given by

$$D_L(s) = \frac{R_6}{R_5(1 + R_6C_6s)}\frac{R_4C_3s}{1 + R_4C_4s} \tag{22}$$

where

$$R_4C_4 = R_6C_6 = \frac{T_d}{2\pi} = 2 \times 10^{-4} \text{ s}$$

and

$$\frac{R_6R_4C_3}{R_5} = k' = \frac{5}{41} \text{ s}. \tag{23}$$

Therefore, (22) becomes

$$D_L(s) = k'\frac{s}{\left(\frac{Td}{2\pi}s + 1\right)^2} \tag{24}$$

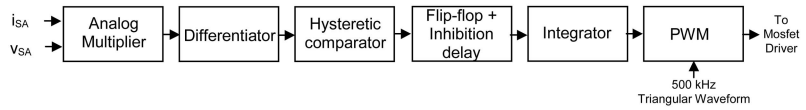

Fig. 6. Extremum-seeking control-based MPPT.

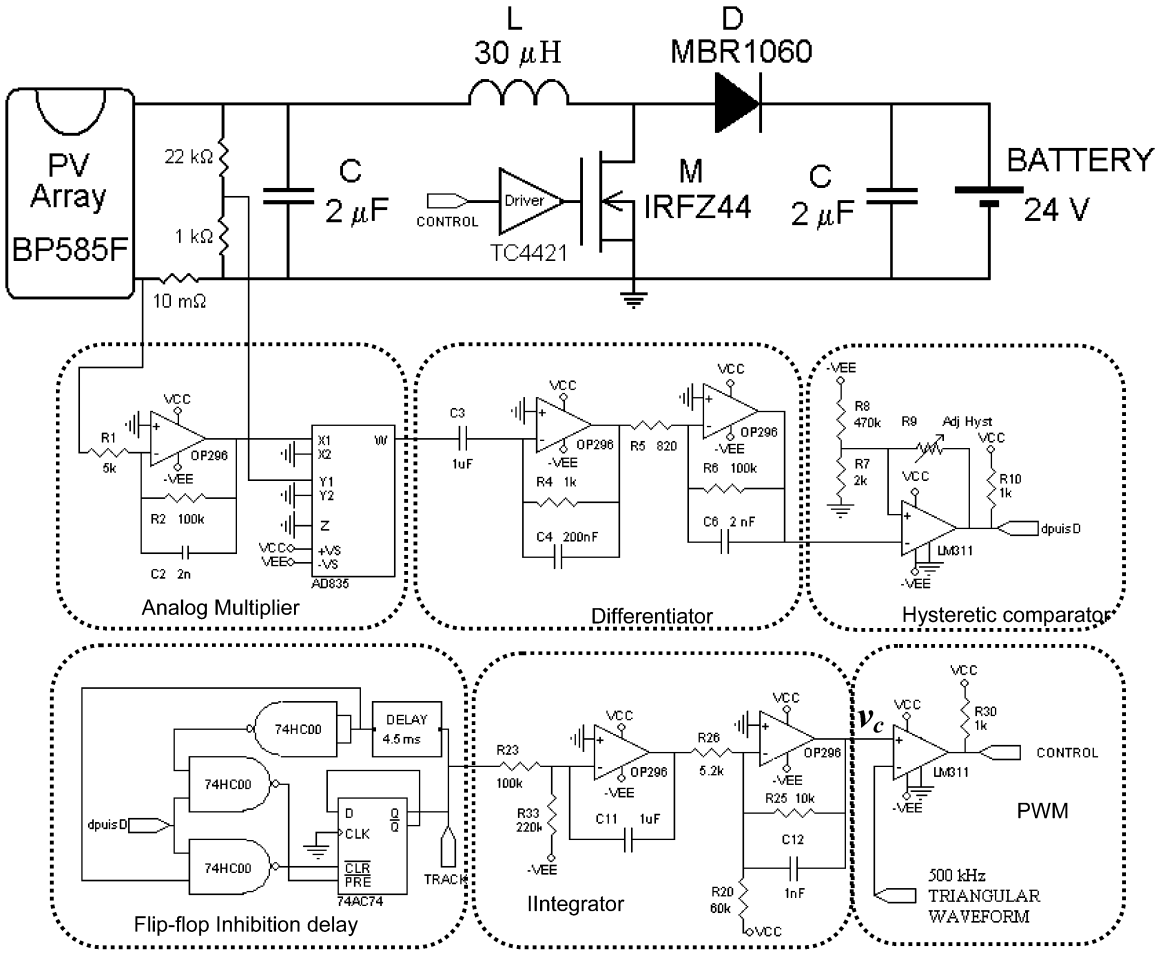

Fig. 7. Practical implementation of PV system with extremum-seeking control-based MPPT.

where Td has been tuned to $Td = T_{\mathrm{MPPT}}/8$, T_{MPPT} being the oscillation period around the maximum power point that characterizes the MPPT behavior.

It can be observed that $D_L(s)$ is a pure differentiator for signals with frequency contents below $2\pi/Td$. Note, also, that the differentiator rejects the high-frequency noise and the switching ripple due to the transfer function amplitude decrease of -20 dB/decade for frequencies beyond $2\pi/Td$.

Constant Td must be smaller than the converter time-constants which, in turn, must be much bigger than the switching period. The output signal of the differentiator is then processed by a hysteretic comparator which completely eliminates the high-frequency harmonics. The comparator output provides a digital signal which indicates whether the power time-derivative is positive or negative. The digital signal is introduced into a flip-flop with inhibition delay which establishes, after a fixed time interval of 4.5 ms, if the direction of maximum searching has to be maintained or should be changed. The waiting interval ensures that the converter is operating in steady-state when the decision on the change or maintenance of the control law sign is made. The 4.5 ms interval is four times bigger than the largest time-constant of the converter in order to guarantee that the converter transients do not affect the tracking operation. The output signal of the flip-flop is multiplied by a constant α and the result is integrated in order to obtain the ramp signal required by the modulator input of the switching converter. The voltage excursion Δv_{SA} around the maximum power point is given by $\Delta v_S \approx \alpha \cdot T_{\mathrm{MPPT}}/2$ and it will eventually establish the MPPT efficiency [19]. Observe that the mentioned voltage excursion can be viewed as a chattering that would only disappear in the ideal case of zero inhibition delay.

C. Electronic Implementation

The block diagram depicted in Fig. 4 has been implemented as shown in Fig. 7 where the complete converter and its control circuit are depicted in detail. The PV generator is a solar array of monocrystalline cells with a nominal open-circuit voltage v_{OC} of 22.1 V and a nominal voltage value at the maximum power point of 18 V. Since the load is a 24 V acid-lead battery, the dc-to-dc conversion must be performed by a boost structure. The control circuit for the MPPT function consists of six blocks, namely, analog multiplier, differentiator, hysteretic comparator, flip-flop with inhibition delay, integrator, and pulsewidth modulator. The analog multiplication is performed by the IC AD835 whose two inputs are proportional to current and voltage of the PV array, respectively. The output of the analog multiplier provides a signal proportional to the array power which is then differentiated by a linear circuit of two operational amplifiers implementing the transfer function (28). The double-pole of such transfer function is located almost one decade above the expected oscillation frequency of the array voltage around the maximum power point. The sign function of the panel power is subsequently obtained by means of a hysteretic comparator based on the LM311 voltage comparator. The high level output of the comparator (5 V) corresponds to a negative time-derivative of the panel power while the low level (0 V) is the response to a positive derivative. The output of the comparator constitutes the input of a logic circuit based on the IC 74AC74 acting as R-S flip-flop. The generation of a ramp signal with slope $\pm\alpha$ is implemented by means of the integrator connected at the output of the flip-flop. The integral function is performed by the cascade connection of an inverting integrator and an inverting amplifier. The high level (5 V) of the flip-flop output, combined with a negative offset at the input of the inverting integrator, results in a positive slope α for the ramp at the output of the inverting amplifier. Similarly, the load level (0 V) of the flip-flop output and the negative offset at the input of the inverting integrator leads to a negative slope $-\alpha$. Finally this ramp signal $D(t)$ is compared with a triangular waveform of a 500 kHz to generate the pulsewidth modulation required by the converter operation.

IV. EXPERIMENTAL RESULTS

It is shown in this section the experimental behavior of i_{SA}, v_{SA}, p_{SA} of the PV generator with the proposed MPPT algorithm under different operating conditions. The experimental prototype corresponds to the circuit configuration of Fig. 7 using a PV panel of 85 W of nominal power. All variables have been measured by means of a Tektronix oscilloscope (TDS5104). The current of the PV array has been obtained by means of Tektronix current probe (TCP202).

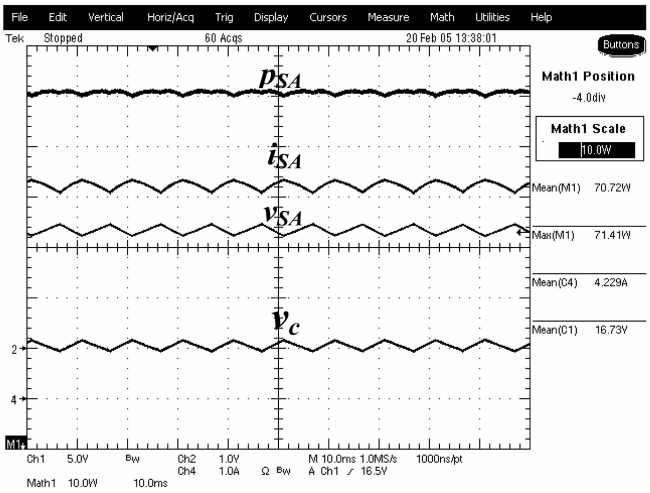

Fig. 8. Steady-state behavior of PV array variables.

A. Steady-State Measurements

Fig. 8 illustrates the steady-state behavior of the different variables at the input port of the PV system depicted in Fig. 7. Note that signal v_c has been also represented. This signal is compared with the triangular waveform in order to obtain PWM control and to eventually determine the duty cycle. Current and voltage of the PV array are 180° out of phase as it can be expected from the i-v characteristics of the PV module. The frequency of the instantaneous power p_{SA} is twice the frequency of current or voltage. Therefore, each half period of current or voltage, a maximum value of p_{SA} is reached. As predicted by the analysis in Section III, a linear increase in time of the duty cycle produces a linear decrease of the PV array voltage and vice versa. As shown in the information displayed at the right part of the figure, the average value of p_{SA} is 70.72 W for a maximum value of power of 71.41 W, which results in a MPPT efficiency [19] of 99.0%.

B. Start-Up

The transient behavior of the PV array variables during start-up are shown in Fig. 9. Starting from an initial state corresponding to the array open-circuit voltage (v_{OC} = 22 V, i_{OC} = 0 A), voltage v_{SA} decreases with constant slope during the transient-state while power p_{SA} increases. Since the time-derivative of the power is positive, no changes at the flip-flop output take place. The first change of the system state, i.e., voltage v_{SA} increasing with constant slope, takes place instantaneously after reaching the first maximum power point. However, the successive changes of state will occur if the maximum power point has been

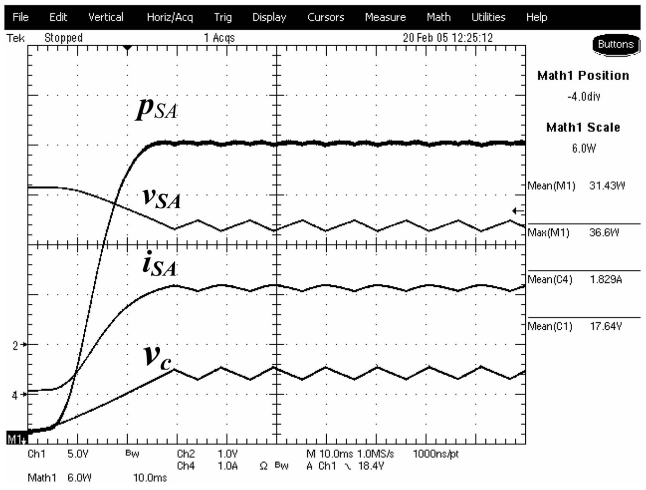

Fig. 9. Start-up from open-circuit.

reached, and a minimum time of 4.5 ms has elapsed since the last state change. It can be also observed that in steady-state the slope change in both current and voltage takes place between two maxima of power p_{SA}, because the frequency of the power waveform is twice the frequency of current and voltage.

C. Input Perturbations

Two experiments have been performed in order to check the response of the PV system with MPPT control to input perturbations. In the first case, abrupt changes in panel current have been produced by the successive connection and disconnection of two PV panels in parallel. In the second case, a 5 V dc source in series with the PV generator, has been successively connected and disconnected in order to provoke a voltage shifting of the *v-i* characteristics of the solar array. Abrupt changes as those produced in the first experiment take place regularly in satellites as, for example, on the one hand, in the regular operation of power system configurations based on the sequential-switching regulator concept or, on the other hand, in the sudden increase of the solar array characteristics intending to avoid the "lock-up" mechanism at the end of eclipses in sunlight regulated-voltage topologies [17]. The aim of the second experiment is to approximately reproduce the effect of the temperature variation in the *v-i* characteristics of the PV panel since one of the main consequences of such variation, among others, is the voltage shifting of the *v-i* curve [18].

1) *Array Paralleling*: Fig. 10(a) shows the behavior of the panel variables after the connection of an additional panel in parallel with the PV generator. As it can be expected, the current increases while the voltage remains practically unchanged excepting the transient-state connection. Since the voltage operating point around the maximum power point of one panel has not changed, the new maximum power point is almost instantaneously reached. A similar situation is observed in Fig. 10(b) when the panel added previously is removed.

2) *DC Voltage Source in Series with PV Generator*: Fig. 11(a) shows the behavior of the panel variables after the insertion of a 5 V dc voltage source in series with the PV generator. In this case, the voltage operating point around the maximum power point has changed, and therefore, the MPPT has to adapt the system operation to the new situation. Thus, the array voltage increases linearly until reaching a maximum power point 32 ms after the introduction of the voltage perturbation. Similarly, after disconnecting the dc voltage source, a linear decrease of the array voltage occurs and the new operating point is reached 20 ms later.

V. CONCLUSIONS

An MPPT system based on extremum-seeking control has been developed. The MPPT algorithm reported here guarantees the stability of the maximum

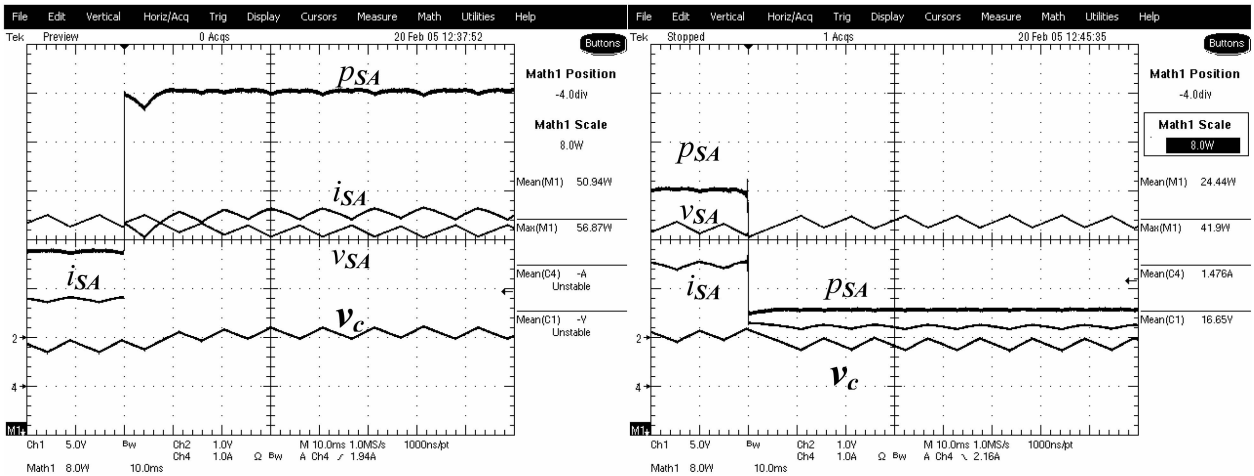

Fig. 10. Response to parallel connection of an additional panel. (a) Connection. (b) Disconnection.

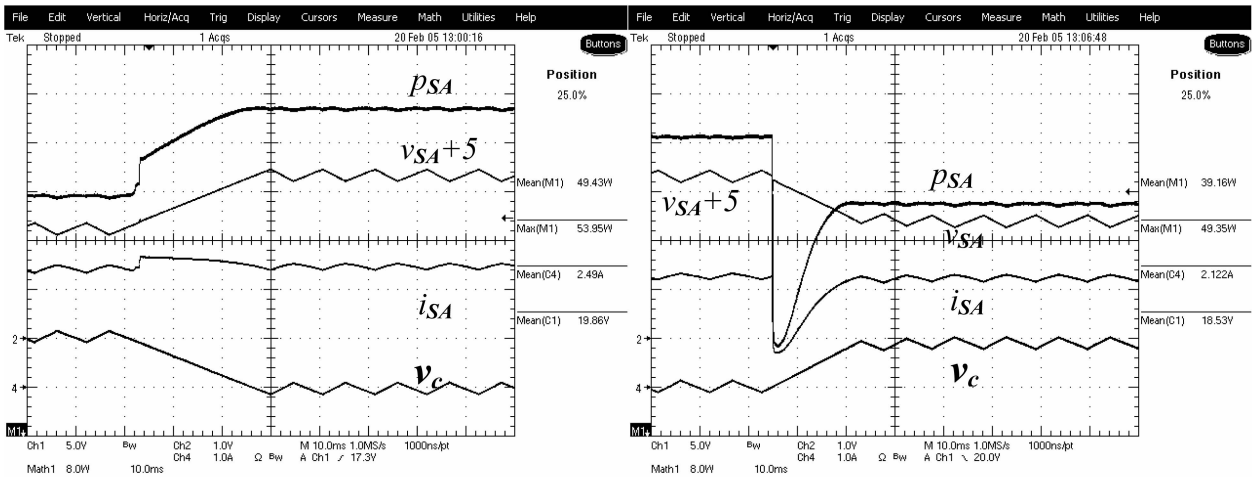

Fig. 11. Response to series connection of additional 5 V dc source. (a) Connection (b) Disconnection.

seeking procedure for large-signal operation. The theoretical predictions have been experimentally validated in a PV system consisting of a standard array, a boost converter, and a 24 V battery as a system load. Further research contemplates the use of the MPPT algorithm in other PV systems, i.e., PV systems supplying different loads through different converters. Also, the combination of the MPPT algorithm and state-feedback control is in progress.

REFERENCES

[1] Enslin, J., Wolf, M., Snyman, D., and Swiegers, W.
Integrated photovoltaic power point tracking converter.
IEEE Transactions on Industrial Electronics, **44** (Dec. 1997), 769–773.

[2] Noguchi, T., Togashi, D., and Nakamoto, R.
Short-current pulse-based maximum-power-point tracking method for multiple photovoltaic converter module system.
IEEE Transactions on Industrial Electronics, **49** (Feb. 2002), 217–223.

[3] Wyatt, J., and Chua, L.
Power theorem, with solar application.
IEEE Transactions on Circuits and Systems, **30**, 11 (Nov. 1983), 824–828.

[4] Applebaum, J., and Sarma, M. S.
The operation of permanent magnet dc motors powered by a common source of solar cells.
IEEE Transactions on Energy Conversion, **4**, 4 (1989), 635–642.

[5] Ikegami, T., Maezono, T., Nakanishi, F., Yamagata, Y., and Ebihara, K.
Estimation of equivalent circuit parameters of PV module and its application to optimal operation of PV system.
Solar Energy Materials & Solar Cells, **67** (2001), 389–395.

[6] Veerachary, M., Senjyu, T., and Uezato, K.
Feedforward maximum power point tracking of PV systems using fuzzy controller.
IEEE Transactions on Aerospace and Electronic Systems, **38**, 3 (July 2002), 969–981.

[7] Gow, J., and Manning, C.
Controller arrangement for boost converter systems sourced from solar photovoltaic arrays or other maximum power sources.
IEE Proceedings Electric Power Applications, **147** (Jan. 2000), 15–20.

[8] Salameh, Z., and Taylor, D.
Step-up maximum power point tracker for photovoltaic arrays.
In *Proceedings of the Annual Meeting of American Solar Society*, Cambridge, MA, June 20–24, 1998, 409–414.

[9] Sullivan, C. R., and Powers, M. J.
A high-efficiency maximum power point tracker for photovoltaic arrays in a solar-powered race vehicle.
In *Proceedings of 1993 IEEE Power Specialists Conference* (PESC'93), Seattle, WA, June 20–24, 1993, 574–580.

[10] Ariyur, K. B., and Krstic, M.
Real-Time Optimization by Extremum-Seeking Control.
New York: Wiley, 2003.

[11] Kristic, M.
Performance improvement and limitation in extremum seeking control.
Systems & Control Letters, **39** (2000), 313–326.

[12] Tse, K. K., Ho, M. T., Chung, H. S., and Hui, S. Y.
A novel maximum power point tracker for pv panels using switching frequency modulation.
IEEE Transactions on Power Electronics, **17** (Nov. 2002), 980–989.

[13] Utkin, V. I.
Sliding Modes in Control and Optimization.
New York: Springer-Verlag, 1992.

[14] Astrom, K. J., and Wittenmark, B.
Adaptive Control (2nd ed).
Reading, MA: Addison-Wesley, 1995.

[15] Valderrama, H., Alonso, C., Martinez-Salamero, L., Singer, S., Estibals, B., and Maixe-Altes, J.
AC-LFR concept applied to modular photovoltaic power conversion chains.
IEE Proceedings—Electric Power Applications, **149**, 6 (Nov. 2002), 441–448.

[16] Jantsch, M., et al.
Measurement of PV maximum power point tracking performance.
Presented at the 14th European Photovoltaic Solar Energy Conference, Barcelona, Spain, June 30–July 4, 1997.

[17] Capel, A., O'Sullivan, D., and Marpinard, J. C.
High-power conditioning for space applications.
Proceedings of the IEEE, **76**, 4 (1988), 391–408.

[18] O'Sullivan, D.
Satellite power system topologies.
ESA Journal, **13** (1989), 77–88.

Ramon Leyva received the Ingeniero de Telecomunicación and the Ph.D. degrees from Universidad Politécnica de Cataluña, Barcelona, Spain, in 1992, and 2000, respectively.

He is currently an associated professor at the Departamento de Ingeniería Electrónica, Escuela Técnica Superior de Ingeniería, Universitat Rovira i Virgili, Tarragona, Spain, where he is working in the field of nonlinear control of power converters.

Corinne Alonso received the M.S. degree from the University Paul Sabatier, Toulouse, France, the Ph.D. degree and the H.D.R. degree, from the Institut National Polytechnique de Toulouse, respectively, in 1990, 1994, and 2003.

From 1994 to 1996, she was assistant professor at the ENSEEIHT Engineering School, Toulouse, France. Her research interests were focused on the modeling of GTO and IGBT components for railway applications. Since 1996 she has been an associated professor at the Electrical Engineering Department of the Paul Sabatier University and researcher of the Power Devices Division in the LAAS-CNRS. Her research is focused on renewable energies, in particular, photovoltaic conversion, and also on passive component integration.

Isabelle Queinnec received her Ph.D. degree and H.D.R. degree in automatic control in 1990 and 2000, respectively, from the Paul Sabatier University, Toulouse, France.

She is currently researcher at LAAS-CNRS. Her research interests include constrained control and robust control of processes, especially biochemical and environmental processes.

Since 2002 Dr. Queinnec serves as a member of the IFAC technical committee on control of biotechnological processes.

Angel Cid-Pastor graduated as Ingeniero en Electrónica Industrial in 1999 and as Ingeniero en Automática y Electrónica Industrial in 2002 at Universitat Rovira i Virgili, Tarragona, Spain. He received the M.S. degree in design of microelectronics and microsystems circuits in 2003 from Institut National des Sciences Appliquées, Toulouse, France.

He is presently working towards the Ph.D. degree at Laboratoire d'Analyse et d'Architecture des Systèmes LAAS-CNRS, Toulouse, France. His research interests are in the field of power electronics and renewable energy systems.

Denis Lagrange was born in St. Etienne, France, in 1958. He received the Engineer Degree in electrotechnics from ENSEEIHT, Toulouse, France, in 1981.

He has worked as an engineer for the CNRS since 1988 and particularly with LAAS since 2001.

Luis Martínez-Salamero received the Ingeniero de Telecomunicación degree in 1978 and the Ph.D. degree in 1984, both at the Universidad Politécnica de Cataluña, Barcelona, Spain.

From 1978 to 1992, he taught circuit theory, analog electronics and power processing at the Escuela Técnica Superior de Ingenieros de Telecomunicación de Barcelona, Barcelona, Spain. From 1992 to 1993, he was a visiting professor at the Center for Solid State Power Conditioning and Control, Department of Electrical Engineering, Duke University, Durham, NC. From 2003 to 2004, he was a visiting scholar at the Division of Power Devices and Power Integration of the Laboratory of Architecture and Systems Analysis (LAAS), National Agency for Scientific Research (CNRS), Toulouse, France. Since 1995 he has been a full professor with the Departamento de Ingeniería Electrónica, Eléctrica y Automática, Escuela Técnica Superior de Ingeniería, Universitat Rovira i Virgili, Tarragona, Spain, where he is in charge of the Research Group in Industrial Electronics and Automatic Control (GAEI). His research interest is in the field of structure and control of power conditioning systems, namely, electrical architecture of satellites, boats and vehicles, nonlinear control of converters and drives, and power conditioning for renewable energy.

Dr. Martínez-Salamero is the coauthor of more than 50 papers in the fields of modeling, simulation, and control of power converters, and he holds a U.S. patent on dual voltage electrical distribution in vehicles. He was guest editor of the *IEEE Transactions on Circuits and Systems Special Issue on Simulation, Theory and Design of Switched-Analog Networks* (Aug. 1997). He organized the 5th European Space Power Conference (ESPC'98) in cooperation with the European Space Agency. He served during two terms (1996–2002) as a dean of the School Engineering of Universitat Rovira i Virgili, Tarragona, Spain. He was distinguished lecturer of the IEEE Circuits and Systems Society in the period 2002–2003.